



## Pore Type Inversion and S-Wave Velocity Estimation for the Characterization of Salawati Carbonate Reservoir

M. SYAMSU ROSID<sup>1</sup>, YOGI MULIANDI<sup>1</sup>, and AL HAFEEZ<sup>2</sup>

<sup>1</sup>Department of Physics, Universitas Indonesia

<sup>2</sup>J.O.B PERTAMINA-Petro China Salawati

Corresponding author: [syamsu.rosid@ui.ac.id](mailto:syamsu.rosid@ui.ac.id)

Manuscript received: May, 18, 2018; revised: July, 15, 2019;  
approved: September, 8, 2020; available online: March, 29, 2021

**Abstract** - A rock physic study was conducted in Salawati Basin, Papua, Indonesia. This field produces hydrocarbons from coral reef formation. The carbonate reservoir has a very heterogeneous and complex pore type. This study used data from ten wells. Two wells (K-2 and Z-1) have Vs data, while the other eight do not. This study was done to identify the pore type of the reservoir rock, and to estimate the Vs log data in this area. The characterization of the carbonate reservoir was carried out using the DEM (Differential Effective Medium) inversion method. In calculating the bulk ( $\kappa$ ) and shear ( $\mu$ ) modulus, the DEM method is supported by the HSW (Hashin-Shtrikman-Walpole) formula in the form of its rock matrix model and Gassmann's relation for its fluid contents. The inversion results show that in eight wells the reservoir is dominated by crack pore type, and in the other two wells the reservoir is dominated by stiff pore type. As for the Vs data, at reference wells K-2 and Z-1, the estimated Vs corresponds very well to the actual Vs, with RMS error of less than 2 m/s and 3 m/s respectively. Another qualitative verification shows that the pore type inversion results are almost perfectly consistent with thin-layer lithology data.

**Keywords:** carbonate reservoir, Hashin-Shtrikman-Walpole (HSW), modified DEM, S-wave velocity, Salawati Basin

© IJOG - 2021

### How to cite this article:

Rosid, M.S., Muliandi, Y., and Al Hafeez, 2021. Pore Type Inversion and S-Wave Velocity Estimation for the Characterization of Salawati Carbonate Reservoir. *Indonesian Journal on Geoscience*, 8 (1), p.131-146.  
DOI: [10.17014/ijog.8.1.131-146](https://doi.org/10.17014/ijog.8.1.131-146)

### INTRODUCTION

Carbonate-dominated fields nowadays contribute as much as half of the world total hydrocarbon lifting volume. However, the main challenge that engineers and geoscientists alike often face is the fact that carbonate rocks are notoriously elusive to characterize completely. Carbonate reservoir space formed throughout the entire deposition process, the dissolubility, and instability of carbonate reservoirs. It makes the evolution of their pore spaces complicated. Pore type varies over small distances and multiple

pore types exist in the same formation. Pores are often affected and reformed by multiple factors. Carbonate rocks have a variety of pore types, such as moldic, vuggy, interparticle, intraparticle, and fracture (Verwer *et al.*, 2010). Unlike clastics and sandstone that are easier to characterize through several established theories, for example the Xu-White theory (1995), carbonate rocks require scientists to layer many theories to better approximate carbonate pore types. Accurate calculations of carbonate pore types are invariably important, because seismic responses depend quite heavily

on the pore types of a carbonate rock (Cheng and Toksoz, 1979; Wang, 2001; Rosid *et al.*, 2020). The idea to model carbonate rock as having multiple pore types, represented by a value known as aspect ratio and inclusions, is first introduced by Xu and Payne (2009). It is an extension to the earlier Xu-White theory for sandstone. A notable change is the introduction of the concept of secondary pore type, complement to the primary pore type exists in all rocks, namely interparticle pore. Secondary pore types of interest in the case of carbonate rocks are stiff and crack/microcrack (Zhao *et al.*, 2013; Rosid *et al.*, 2018).

The knowledge of pore type compositions in a particular reservoir helps better estimate several parameters used in seismic processing and rock physic analysis, for example bulk modulus and shear modulus. From these parameters, it can be derived several other parameters, such as Lambda-Mu-Rho (LMR), compressional velocity ( $V_p$ ), and shear velocity ( $V_s$ ). These derivative parameters hold an important role in advanced seismic interpretation methods, such as Extended Elastic Impedance (EEI), Amplitude versus Offset/Angle (AVO/AVA), and seismic inversion.

Advances in logging technologies allow geoenvironmental engineers to measure shear velocity ( $V_s$ ) directly from a wellbore using a method like the Dipole Shear Sonic Imager (DSI) from Schlumberger. However, the relative newness of this method is comparable to the traditional sonic logging for compressional velocity ( $V_p$ ) which means that this method is still multiple times more expensive to run. On top of that, old wells, either dry or producing ones, almost always do not have such logging in place. Thus, if one wants to gather shear velocity data, he/she needs to run DSI, which is of course not economically and technically feasible citing various reasons. Hence, an accurate estimation is needed to build  $V_s$  log data from existing parameters.

### General Geology of the Salawati Basin

Many studies were done in the eastern Indonesia region, in a field overlying the Salawati Basin. The field mainly produces carbonaceous

formation known as the Kais Formation with the approximate age of Miocene. Geographically, Salawati Basin is located in the vicinity of Salawati Island, Papua Bird Head. The Salawati Basin has been explored and exploited since early 1900s. Figure 1 shows the general position of the Salawati Basin and its tectonic setting. Figure 2 shows the regional stratigraphy of the Salawati Basin.

The Kais Formation is a carbonaceous formation as a result of reef growth. This formation grew on the top of another carbonate platform known with the same name of the Kais Formation. This carbonate platform is a result of seawater transgression that deposited carbonate-rich minerals in the basin. Overall, the formation of the entire Kais Formation can be summarized into three major events, corresponding to local seawater transgression and regression events. These entire events took place within the timeframe of Miocene only, after which, the deposition of Klasafet Formation with shale-sand properties effectively terminates the growth of the Kais Formation carbonate.

The Kais Formation in the Salawati Basin is subject to the same secondary pore type classifications (Choquette and Pray, 1970). In this study, the various secondary pore types are further classified using a parameter known as pore aspect ratio (Xu and Payne, 2009; Zhao *et al.*, 2013). Additionally, the bulk and shear modulus calculations were done using Differential Effective Medium (DEM) model. Figure 3 highlights the important steps carried out, and modifications were done in this study, adapted from (Xu and Payne, 2009).

### Previous Study

This study is more focused on the use of a method for determining the pore type and estimation of rock modulus applied in the Salawati carbonate reservoir. The Differential Effective Medium (DEM) model has been used in several earlier studies with varying levels of success (Bredesen, 2012; Lubis and Harith, 2014; Rosid *et al.*, 2017; Prananda *et al.*, 2019), including a comparative study with Kuster-Toksoz model (Candikia *et al.*, 2017). In these earlier studies,

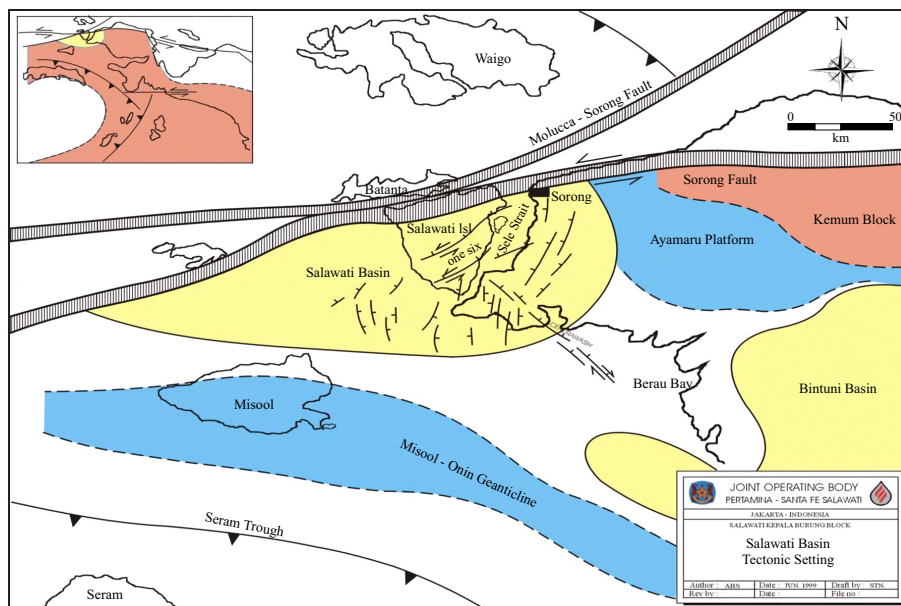


Figure 1. Location of the Salawati Basin and neighbouring structures (Satyana *et al.*, 2002).

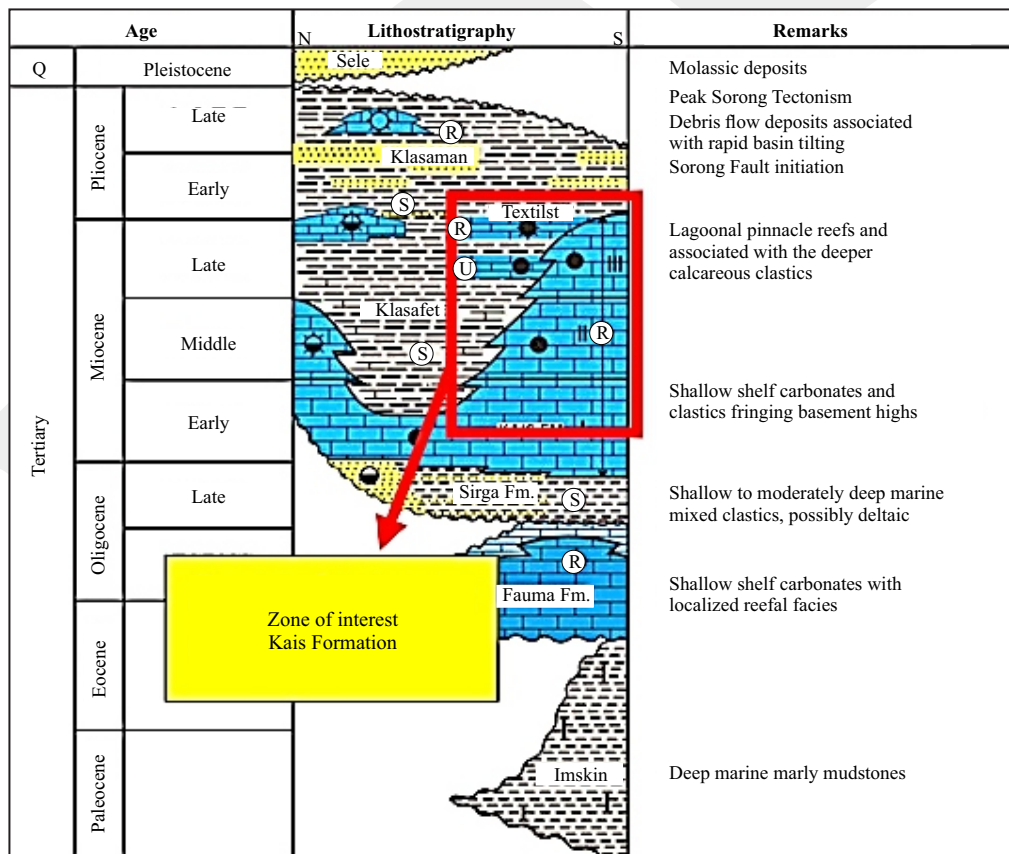


Figure 2. Generalized stratigraphy section and the highlight of the region of interest (Satyana *et al.*, 2002).

the solid rock modelling, which is the first step of the process, was done entirely using Voigt-Reuss-Hill (VRH) model. In this study, the solid

rock modelling was done entirely using Hashin-Shtrikman-Walpole (HSW) model. The VRH model has been a de-facto standard in estimating

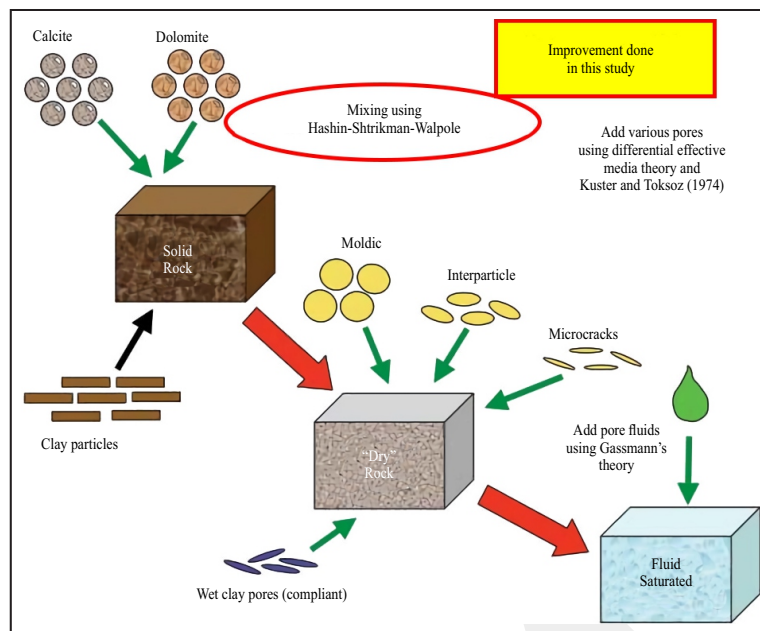


Figure 3. Main steps carried out in this study with improvement highlighted (modified from Xu and Payne, 2009).

bulk and shear modulus of composite materials made up of several independent constituent materials at any concentrations. The main reasons for this widespread use are the ease of calculations owing to a simple formula and well-known basic assumptions used in the model. However, the simplicity of the basic assumptions used leads to a wide range of possible values for bulk and shear modulus predicted by this model and ultimately resulting in lower prediction accuracy (Mavko *et al.*, 2009).

### Improvement Proposed in This Study

The Hashin-Shtrikman-Walpole (HSW) model is an extension of the VRH model by introducing a more robust approach in modelling a composite material. The differences will not be discussed here in detail, as they are readily available in Mavko *et al.* (2009). The HSW model generates a much tighter upper bound compared to the VRH model, resulting in dramatic range reduction and consequently possible values of bulk and shear modulus, leading to a better accuracy compared to the VRH model. A smaller range of values is expected to help lower the standard deviation of the predicted bulk and shear modulus, resulting in lower RMS error in final results. Ye

and Hong (2013) applied the HSW model in the calculation and analysis of carbonate models with different combinations of pore types.

As outlined at the beginning of this paper, advanced seismic interpretation almost always relies on several additional data that unfortunately oftentimes unavailable due to technical reasons such as old or incomplete data or economic reasons such as financially unfeasible to run expensive log on a wildcat, old, or already producing well. Hence, the study aims to close this gap by providing an accurate estimation of these most sought-after data. The additional data namely the shear velocity ( $V_s$ ) log and pore type log, both of which when used properly, may accelerate the finding of pay zones.

### METHODS

In order to achieve the objective, several models and calculations were used. First, several models of the properties of solid rocks composed of several minerals, namely calcite, dolomite, quartz, and clay. The percentage of each constituent was obtained from petrophysical calculations that were done before this study, therefore

outside the scope of this study. The influence of primary and secondary pore types using modified Differential Effective Medium (DEM) incorporated critical porosity cut-off of 60%. Finally, the fluid-saturated rock model using Gassmann theory with pre-processed fluid data was obtained from petrophysical calculations that were done before this study. The results of these steps of DEM inversion are the bulk and shear moduli of fluid-saturated rocks which then can be used to obtain estimated compressional velocity ( $V_p$ ), shear velocity ( $V_s$ ), and pore type log. The processes are shown schematically in Figure 3.

The estimated  $V_p$  data were then compared to the actual/measured  $V_p$  data to minimize differences, hence to estimate error. If possible, when the data are available, estimated  $V_s$  data were first compared to the actual  $V_s$  data to minimize differences. After that, the estimated  $V_p$  data were then compared to the actual  $V_p$  data to ensure consistency. The process of DEM calculations was reiterated continuously until the error was as small as technically possible. To achieve the desired error, in each step, the iteration would add one percent pore type inclusion, either stiff or crack secondary pore type. Inclusion here is the aspect ratio value of the three pore types of interparticles, cracks, and stiffs. If the estimated  $V_p$  is greater than the measured  $V_p$ , then the estimated  $V_p$  is added the inclusion of crack pore type. Vice-versa, if the estimated  $V_p$  is smaller than the measured  $V_p$ , then the estimated  $V_p$  is added stiff pore type inclusions. Only after that, the final bulk and shear moduli and pore type log were extracted and presented as the best estimate for a particular well.

### Overview of data availability

In this study, a total of ten well logs have been obtained. Two well logs, known as K-2 and Z-1, are a complete logs including  $V_s$  data. Therefore, they would be used to calibrate and to verify the method which is indeed correct, and the other eight well logs were used to estimate the  $V_s$  data and pore type logs. Table 1 summarizes this.

## RESULTS AND ANALYSIS

### Reference Well K-2

Figures 4 to 6 show the results of the calculations on the reference Well K-2. Figure 4 left is the actual/measured  $V_p$  log (blue) compared to the estimated  $V_p$  log (red). The result matches almost perfectly, meaning that the estimated  $V_p$  values match very closely to the actual  $V_p$  values obtained from logging. Figure 4 right is the actual/measured  $V_s$  log (blue) compared to the estimated  $V_s$  log (red). The general trend of the estimated values is very close to the general

Table 1. Summary of Well-data Availability (o: provided, and x: unprovided)

Well	Log						
	Depth	Gam- ma Ray	Po- ros- ity	Den- sity	Comp. Sonic	Shear Sonic	Wa- ter Sat.
K - 1	o	o	o	o	o	x	o
K - 2	o	o	o	o	o	o	o
M - 5	o	o	o	o	o	x	o
M - 10	o	o	o	o	o	x	o
M - 20	o	o	o	o	o	x	o
M - 28	o	o	o	o	o	x	o
M - 32	o	o	o	o	o	x	o
S - 5	o	o	o	o	o	x	o
T - 3	o	o	o	o	o	x	o
Z - 1	o	o	o	o	o	o	o

trend of the actual values. RMS error for the  $V_p$  estimation is less than 2  $m/s$  and for the  $V_s$  estimation is less than 100  $m/s$ . This may be seen as an error or inaccuracy in this method, as it only used a few parameters. Thus, this result can be said to be better than expected.

Another way to confirm the matches between the actual data and estimated data can be seen in Figure 5. On the left part, the cross plot shows a very high degree of linearity with almost no outlier, while on the right part, the cross plot shows a high degree of linearity with equal distribution of points to the left and right parts of the trendline.

On the left of Figure 6, it can be seen that the majority of the pores in reference Well K-2 has

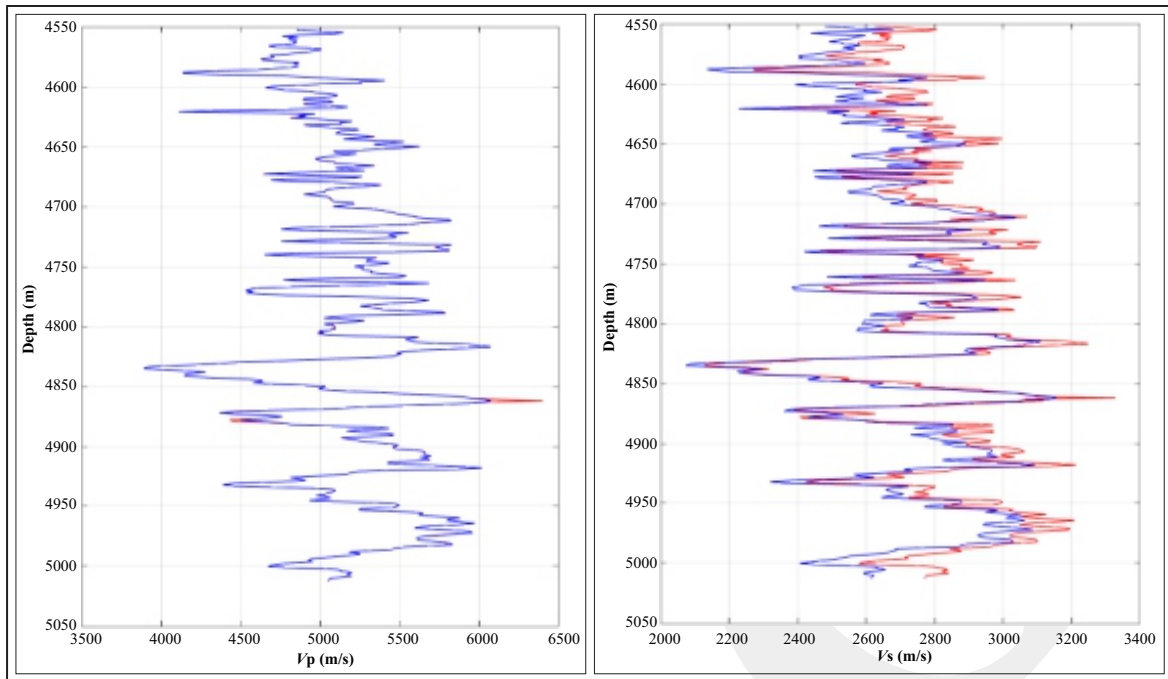


Figure 4.  $V_p$  (left) and  $V_s$  (right) comparison between actual data (blue) and estimated data (red) of Well K-2.

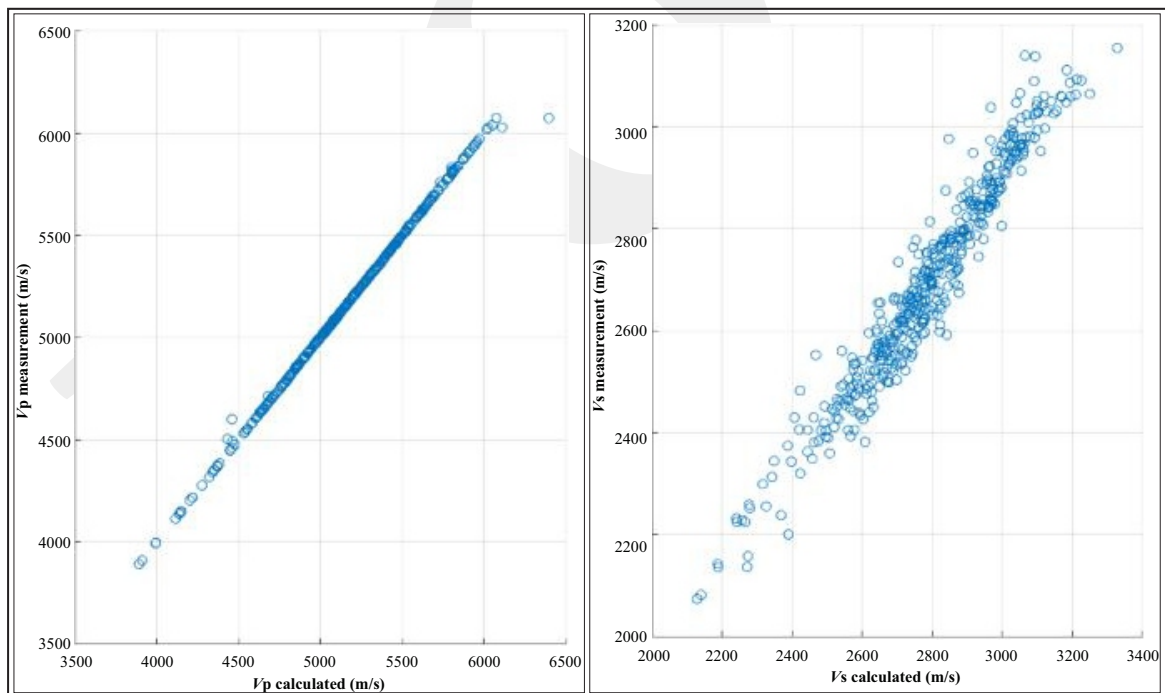


Figure 5.  $V_p$  crossplot (left) and  $V_s$  crossplot (right) confirming high matches between actual data ( $y$ -axis) and estimated data ( $x$ -axis) of Well K-2.

a small aspect ratio of approximately lower than 0.1, and the corresponding interpretation is that this particular well is dominated by crack pore type, although there are several porous zones

indicated by the presence of stiff pores. Indeed, internal DST reports from the company confirmed that at this depth interval there was the presence of hydrocarbons. Overall, the methods used in this

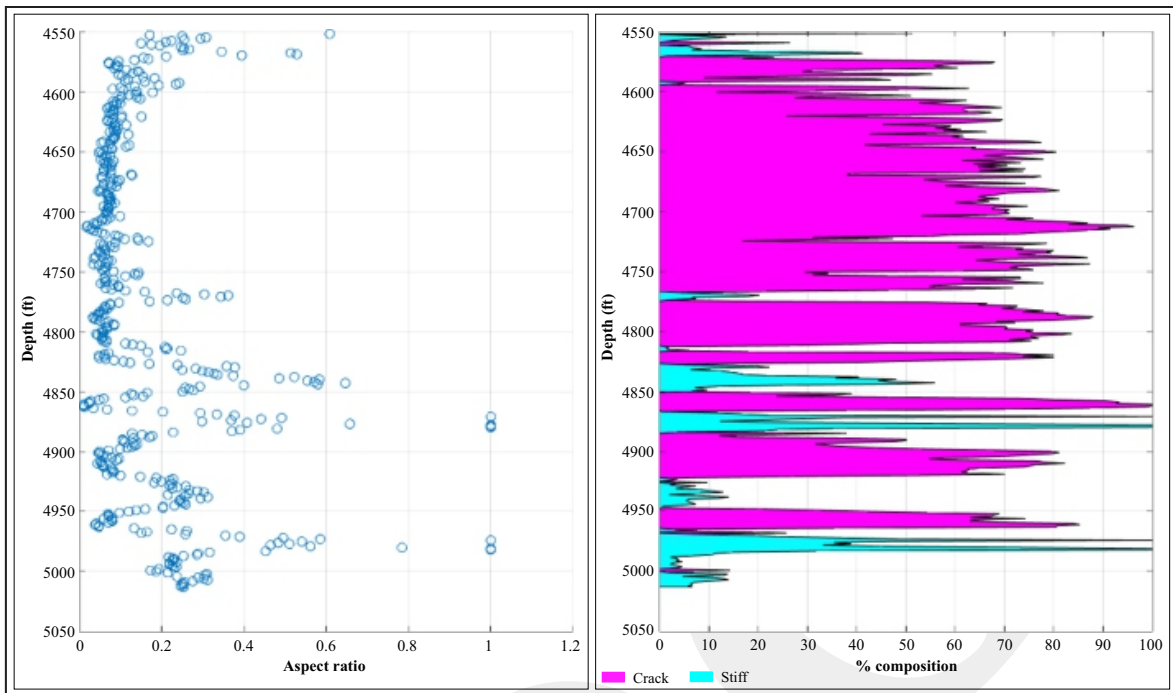


Figure 6. Estimated dominant pore aspect ratio (left) and interpreted crack/stiff pore type composition (right) at Well K-2.

study have been successful in estimating several important physical characteristics of this well.

### Reference Well Z-1

Another well with  $V_s$  data available is known as Z-1. From Figure 7 it is evident that there is a quite handful of estimation errors manifest as spikes. Both  $V_p$  (left) and  $V_s$  (right) estimations are affected by this phenomenon. However, looking past the occasional error, it can be seen that the estimated data (red) match very well with the actual data (blue). Furthermore, these errors are evident in Figure 8, showing as data points that are outside the linear trends, hence counting as outliers.

Earlier possible explanation to this phenomenon was that the algorithms used were not robust enough to handle the particular characteristics of this well. Subsequently, the algorithms were changed to enhance the robustness. However, this approach was not able to achieve stellar results. Therefore, it can be concluded that the algorithms are already sufficient, and this point is proved in all other wells that generate near-perfect estimation.

Another possible explanation is that the well data themselves were somehow not optimally

conditioned. Inferring from a well completion report, it is known that the borehole quality is pretty low, judging from the irregular calliper log and mismatch with the bit size used during drilling. The calliper log is presented in Figure 9. From the calliper log, it is evident that there was an instance of washout during the drilling process, and some of them were quite extensive washout. Generally, washout leads to uneven wellbore and ultimately affects the quality of all subsequent logging processes ran on the well.

Nevertheless, Figure 10 shows that the methods estimate that there are several zones of porous rocks that are most probably able to flow liquids. Indeed, data from DST and thin sections confirm the estimation that the porous regions match well with DST results.

### Results From Other Wells

Aside from the two references Wells K-1 and Z-1, eight other wells do not have shear velocity ( $V_s$ ) data, and suggest the method to estimate these missing data. Several wells are selected to represent the methodability in estimating  $V_s$  and pore type data. It also includes calculated

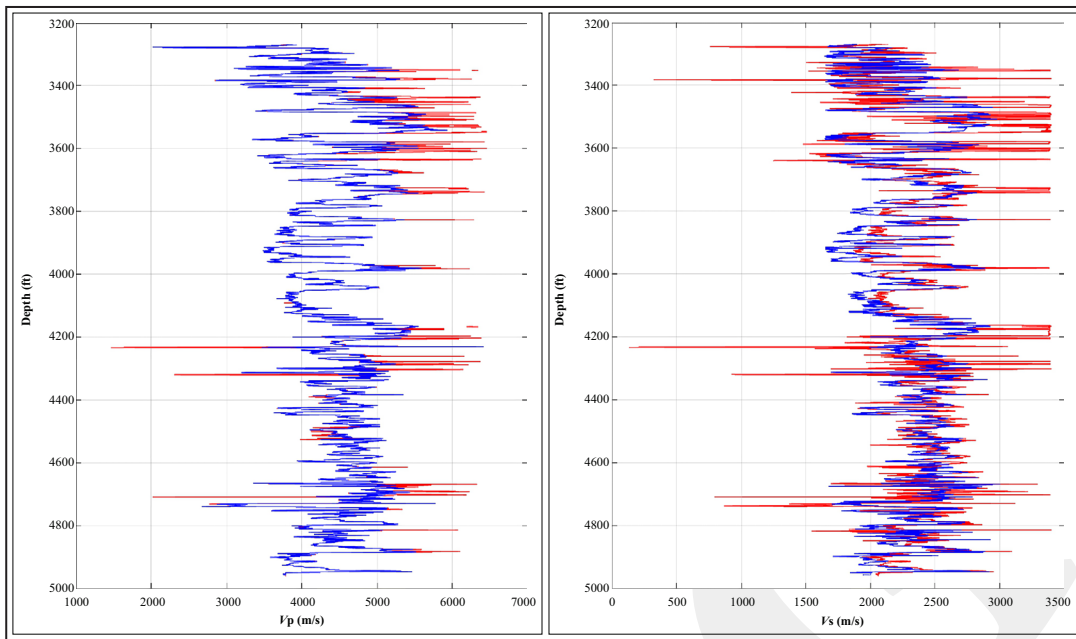


Figure 7.  $V_p$  (left) and  $V_s$  (right) comparison between actual data (blue) and estimated data (red) at Well Z-1.

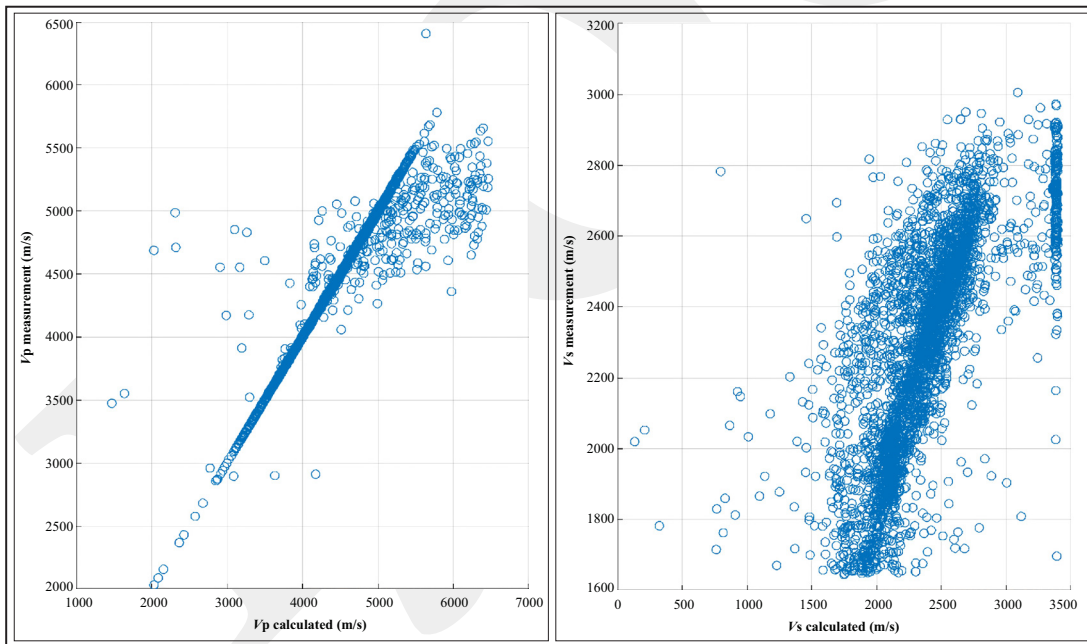


Figure 8.  $V_p$  crossplot (left) and  $V_s$  crossplot (right) confirming high matches between actual data (y-axis) and estimated data (x-axis) at Well Z-1.

$V_p$  RMS error value to quickly determine the quality of the estimation result compared to the actual data.

In well M-5 (Figures 11 and 12), the method was able to near-perfectly estimate the entire  $V_p$  data apart from a small section around 9,520 - 9,530 ft., where the estimate is off by a consid-

erable margin. The method suspected that in this small section there were dense rock layer inserts that were not adequately taken into account, leading to a miscalculation of the estimated data. The porosity log partially confirms the suspicion by indicating very small porosity values, meaning a dense rock layer is present.

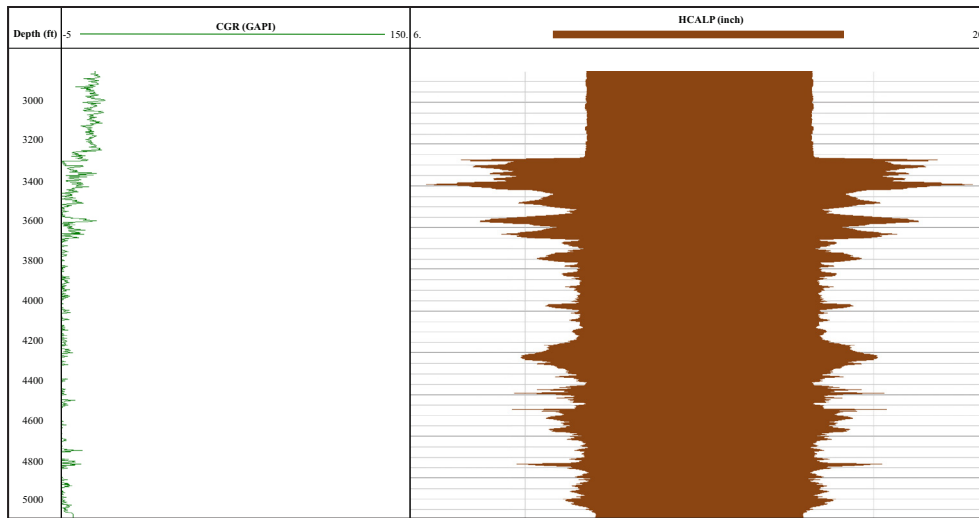


Figure 9. Calliper log (brown) indicating washout zones resulting in less-than-optimal well log data of Well Z-1.

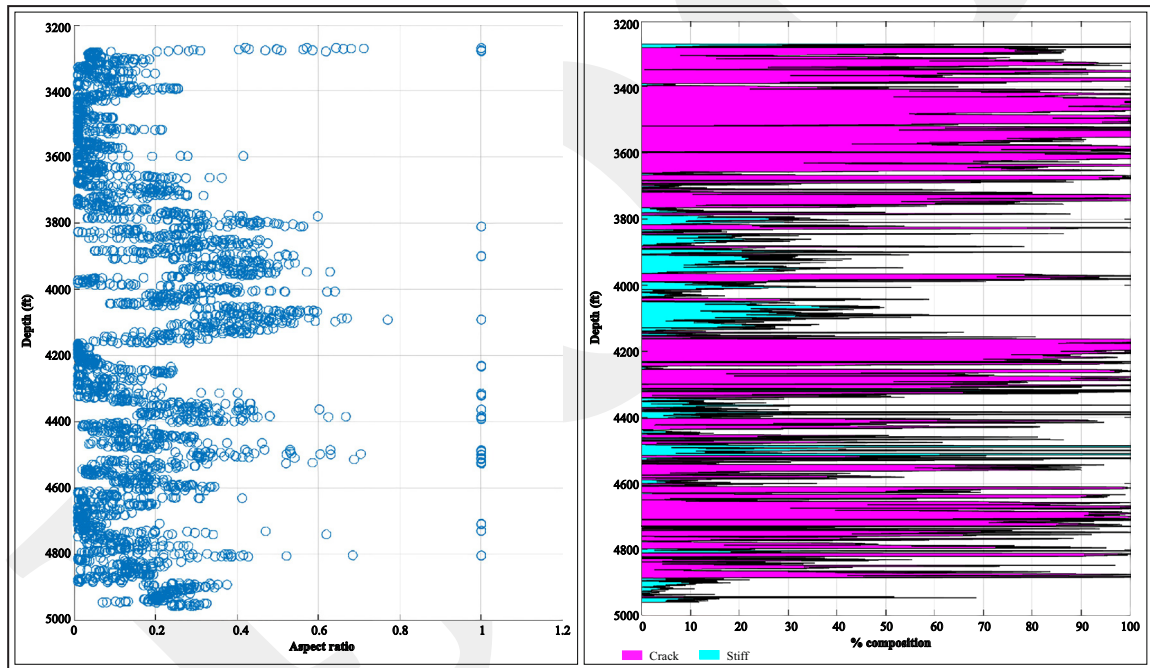


Figure 10. Estimated dominant pore aspect ratio (left) and interpreted crack/stiff pore type composition (right) at Well Z-1.

In well M-10 (Figures 13 and 14), the method was again able to near-perfectly estimate the entire  $V_p$  data, and worth mentioning is that the errors are expectedly very small and only noticeable in very few data points. These errors are most likely caused simply by slightly noisy data in the particular regions, so that in those regions the measured well logs may be off by a certain amount and affecting the calculations in this method.

In well S-5 (Figures 15 and 16), the method was able to perfectly estimate the entire  $V_p$  data without exception. All intervals from the beginning to the end are estimated perfectly with an RMS error of only 0.6  $m/s$ . This means that the method is particularly well-suited for reservoir with similar characteristics to those in S-5 Well.

In well T-3 (Figures 17 and 18), the result of the method closely follows those at Well S-5,

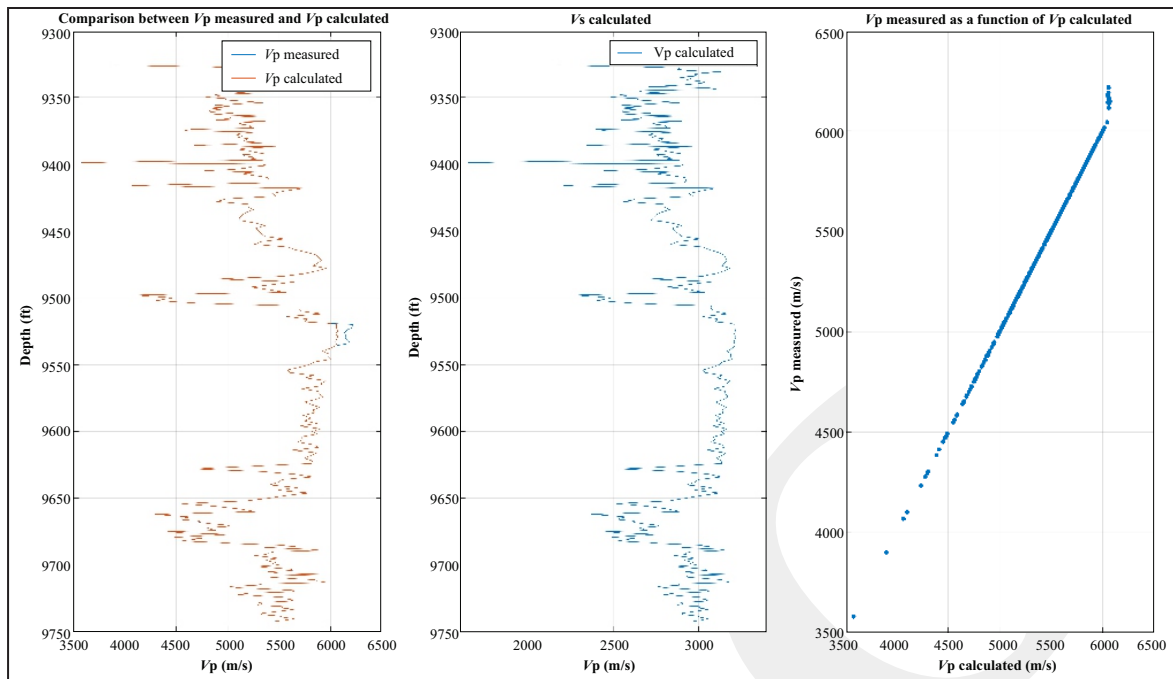


Figure 11.  $V_p$ ,  $V_s$ , and crossplot of actual data (y-axis) and estimated data (x-axis) of Well M-5.

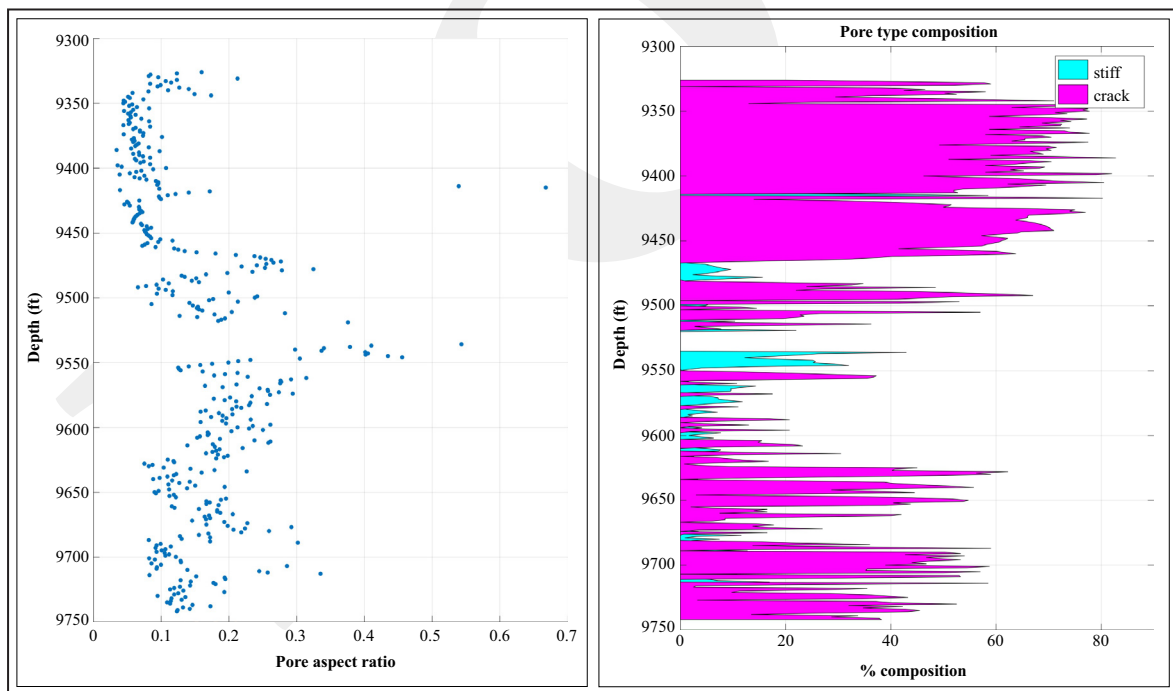


Figure 12. Estimated dominant pore aspect ratio (left) and interpreted crack/stiff pore type composition (right) at Well M-5.

being able to perfectly estimate the entire  $V_p$  data without considerable error. Some errors still exist but at the same magnitude to those at Well S-5, hence the same conclusions apply to this well.

## DISCUSSIONS

Considering the pore type inversion results and  $V_s$  data estimation from all ten wells, it can be seen on the wells that the correlation between

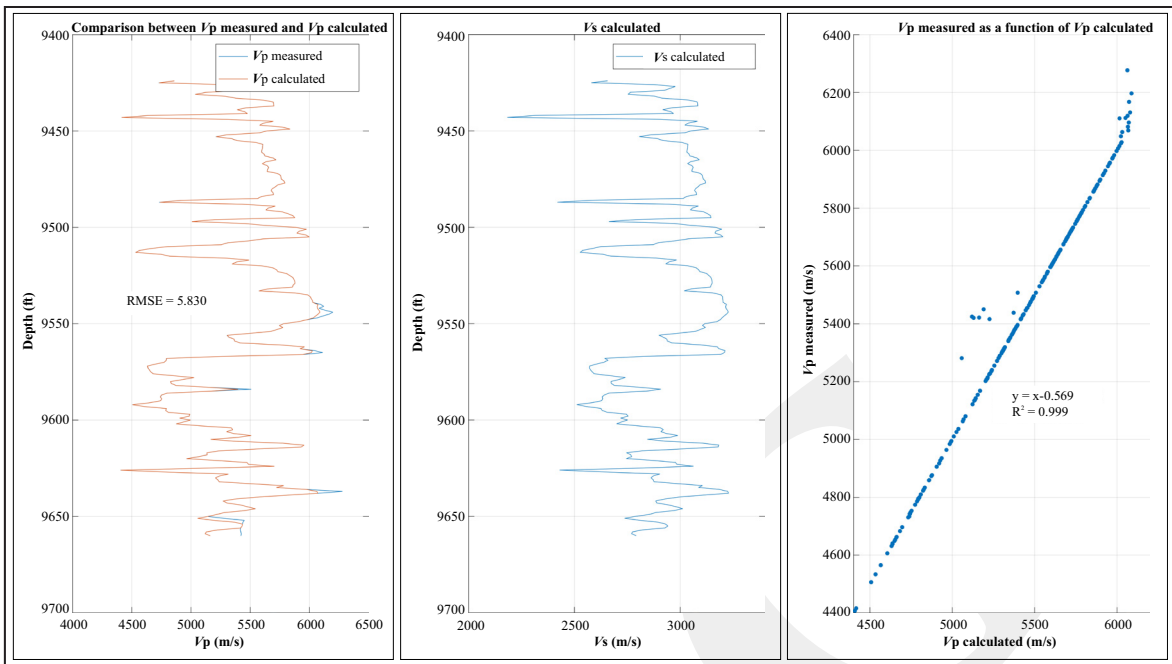


Figure 13.  $V_p$ ,  $V_s$ , and crossplot of actual data (y-axis) and estimated data (x-axis) of Well M-10.

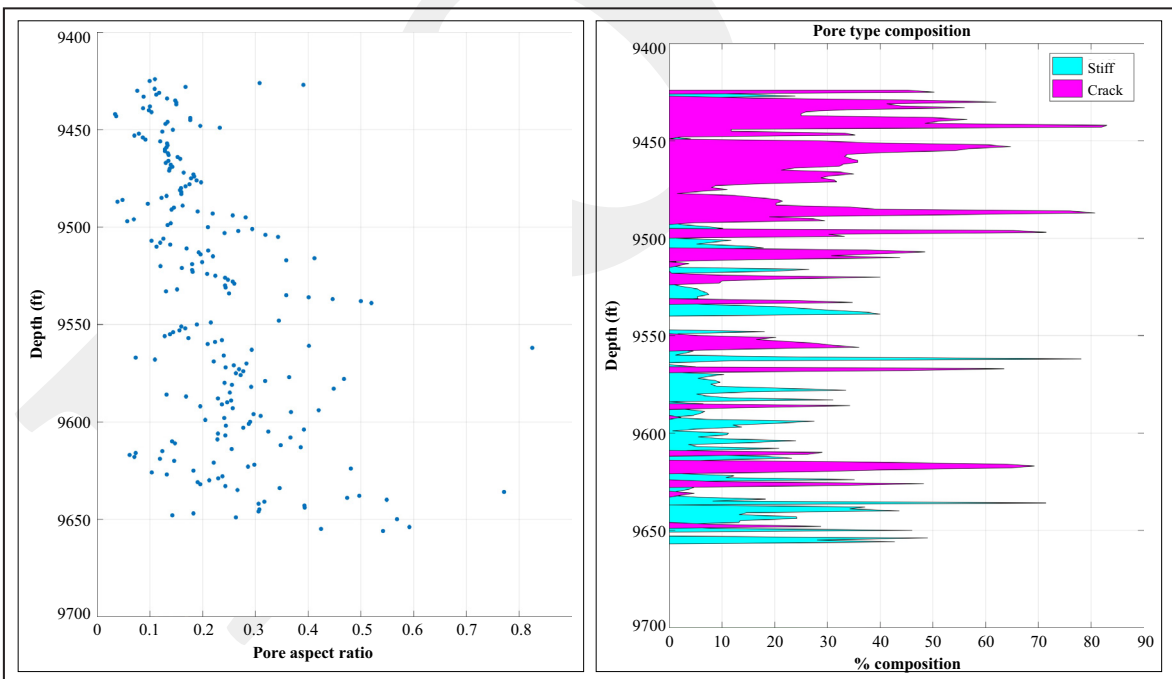


Figure 14. Estimated dominant pore aspect ratio (left) and interpreted crack/stiff pore type composition (right) at Well M-10.

actual  $V_p$  and estimated  $V_p$  data is very close, giving a gradient of one and the correlation coefficient of  $R^2 = 0.999$ , meaning that the estimated  $V_p$  data is indeed near-identical to the actual  $V_p$  data. Specifically, within the datasets of the reference Wells K-2 and Z-1 there are  $V_s$  log data.

These data prove to be invaluable in confirming used results in estimating  $V_s$  log on wells without  $V_s$  data.  $V_s$  log comparison on Well K-2 shown in Figure 4 right is very satisfactory. Thus, it is the case with the cross plot shown in Figure 5 right indicating highly linear relationship, meaning

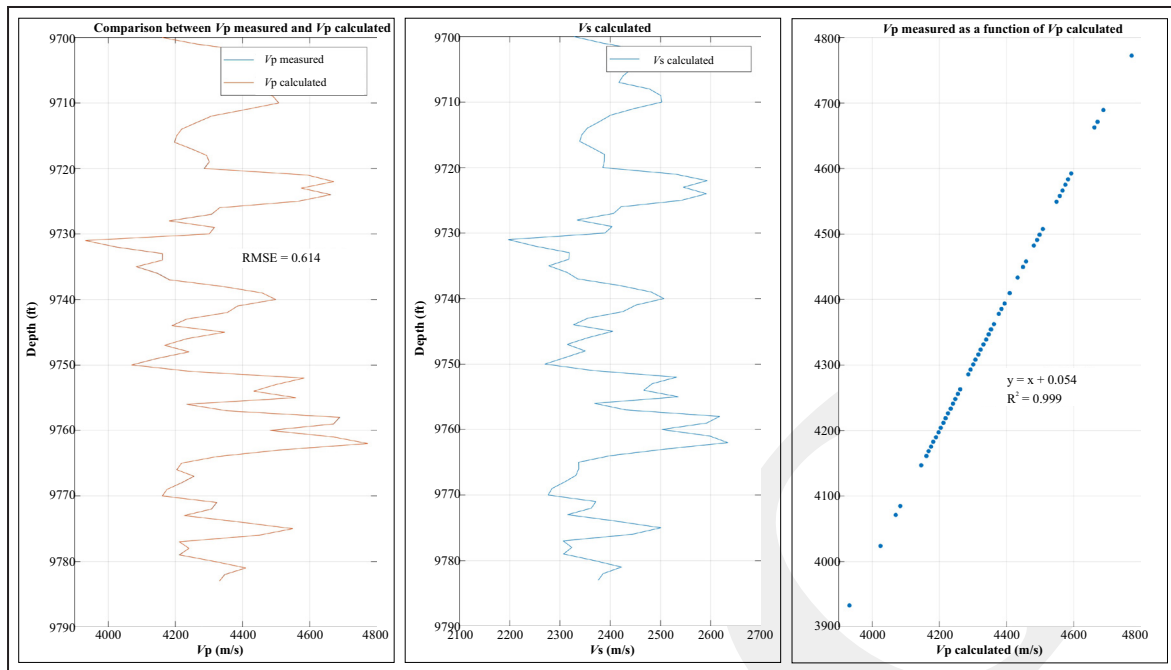


Figure 15.  $V_p$ ,  $V_s$ , and crossplot of actual data (y-axis) and estimated data (x-axis) of Well S-5.

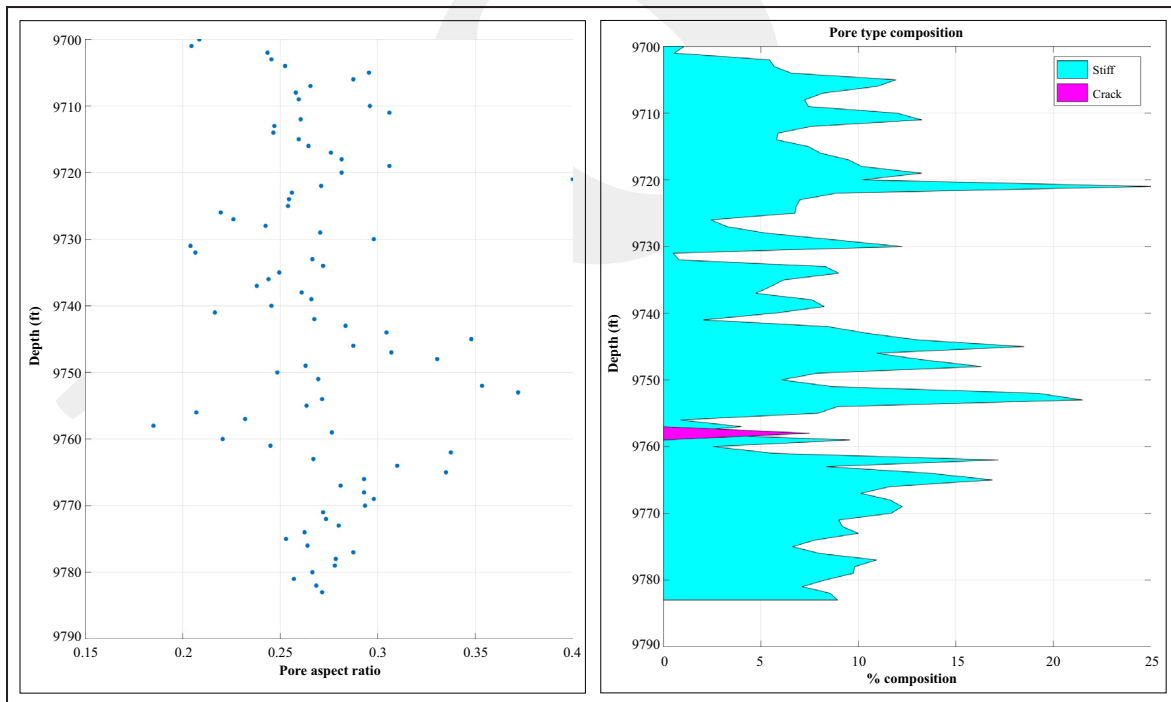


Figure 16. Estimated dominant pore aspect ratio (left) and interpreted crack/stiff pore type composition (right) at Well S-5.

both the actual and estimated  $V_s$  data are very close in value. Since the pores in the carbonate reservoir are heterogeneous, the HSW approach turns out to be more accommodating to rock types that vary nonlinearly.

The high linearity relationship of estimated  $V_p$  to actual  $V_p$  data as well as in the  $V_s$  data and the low RMS error represent the homogeneity conditions of subsurface pore type, either crack or stiff pore type dominated. Most of wells are

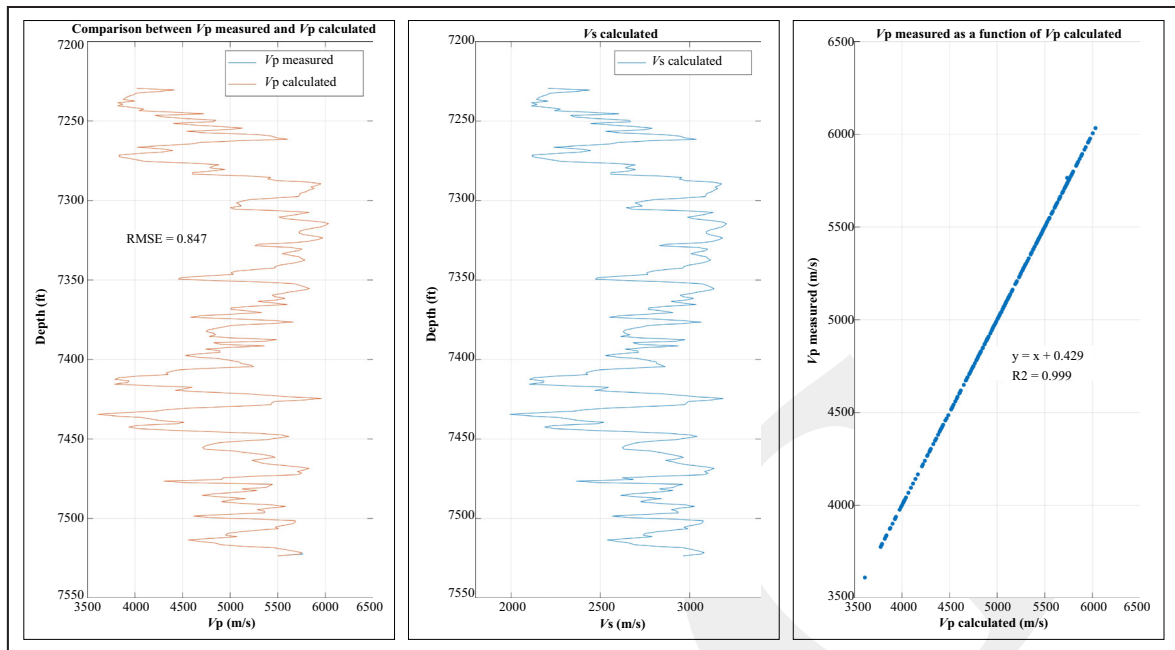


Figure 17.  $V_p$ ,  $V_s$ , and crossplot of actual data (y-axis) and estimated data (x-axis) of Well T-3.

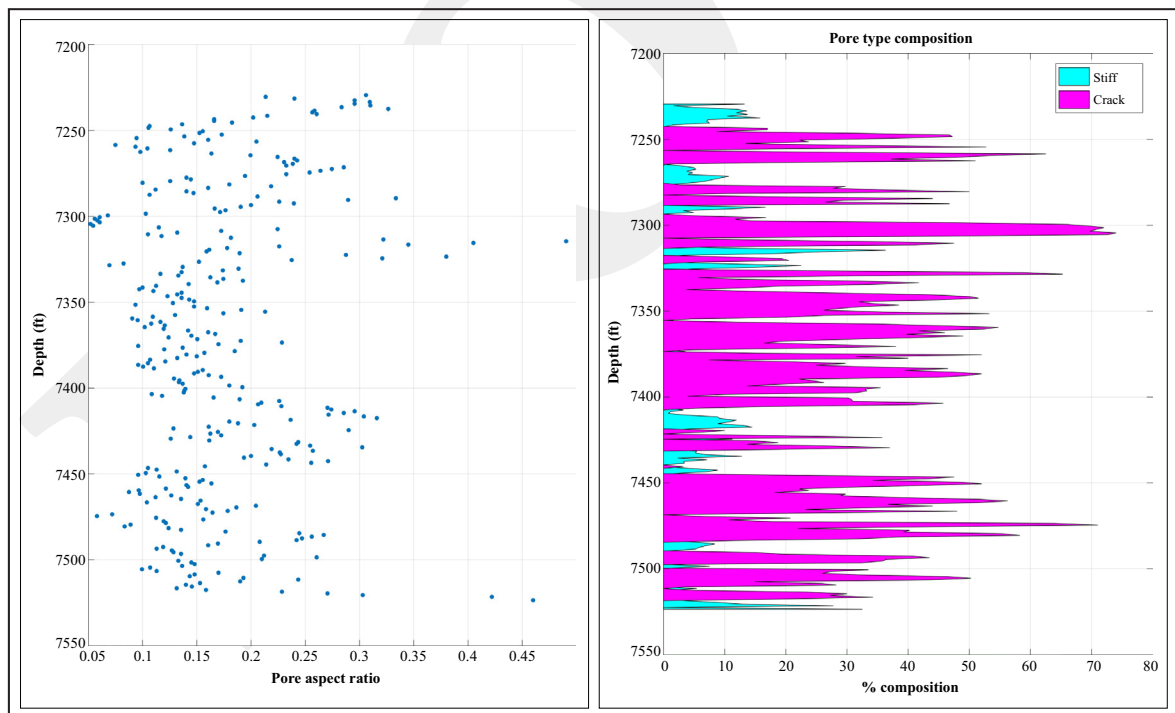


Figure 18. Estimated dominant pore aspect ratio (left) and interpreted crack/stiff pore type composition (right) at Well T-3.

characterized as crack pore type dominated. This is supported by the reality that the oil production of the Salawati Basin is believed to have been controlled by the fracture system. The basin was intensively faulted and most fields are located

within the complex faulted areas (Nurhandoko *et al.*, 2012). Even the fractured zone does not only occurred within the carbonate reservoir but also in the pre-Tertiary Basement with the strike orientation of NE-SW (Pamurty *et al.*, 2016).

The recent study of Prananda *et al.* (2019) is also seismically verified that on the top of Kais Formation the carbonate rocks are present and distributed with relatively high porosity and low acoustic impedance. The study results also show that the deeper the Kais Formation, the smaller the porosity value is.

The Kais Formation is thick carbonates that developed in various environments from lagoonal, bank, to deeper water facies. Therefore, the various types of carbonate sediments were resulted from low energy organic-rich carbonate muds, moderate-high energy reefal carbonates, and fine crystalline carbonates (Satyana *et al.*, 1999). Some wells, like Well S-5, are dominated by stiff pore type. It strongly relates to limestone of Kais Formation with porosity which has been heavily influenced by the diagenetic process, namely the dissolution process by meteoric water. This is indicated by the presence of most porosity cavities, both inter- and intraparticle of rocks in fields that have been filled with sparite and a little limonite, and some have undergone a process of recrystallization presumably due to tectonic processes (Osok, 2019). These processes may also have an impact on the presence of thin layers with varied pore types in Well M-10 as shown in Figure 14.

Meanwhile, on reference Well Z-1, some artifacts are evident, namely spike artifact. On  $V_s$  log, the estimated data is clearly rather noisy with quite a few spikes present on almost the entire depth. However, ignoring the obvious spike, it can be seen that the trend of the estimated  $V_s$  data is actually identical to the trend of the actual  $V_s$  data. This is further cemented by the cross plot in Figure 8 right that shows a relatively large cluster of data points forming a linear trend.

A plausible explanation to the spiking phenomenon on the Well Z-1 may be attributed to the well washout as evident on the caliper (Figure 9). An uneven hole profile may play a big part in affecting the density and porosity log, which in turn affects the method used calculation processes resulting in spiky data. This phenomenon may be mitigated by implementing a despiking algorithm as part of raw

data preprocessing. Postprocess despiking is not recommended as it changes the final result. The spiking phenomenon may also be caused by the existence of high clay content as was also found in the same case by Haidar *et al.* (2018) at different carbonate reservoir fields. The presence of grain size of the silt-clay with clastic texture and layered structure of calcilutite limestone is also verified by Osok (2019) as an element of the Kais limestone.

## CONCLUSIONS

Looking through the entire results, it can be seen that the RMS errors on most wells are very low, except for reference Well Z-1 in which the RMS error cannot be computed due to problematic data. On some wells, the RMS error reaches the region of 0.1 to 1. This means that the difference between actual and estimated data is lower than 1<sup>m</sup>/<sub>s</sub>. From a practical point of view, this is a very good estimation of  $V_p$  and  $V_s$  data. Hence, it can be safely concluded that the method can be used to estimate  $V_s$  with a high degree of accuracy.

Concerning the pore type composition of the wells, of ten total wells, eight wells are dominated by crack secondary pore type. The other two wells are dominated by stiff secondary pore type. This is to be expected in carbonate formations, because differences in the diagenesis environment play a great deal during the formation of secondary pore types.

Finally, although this method is still at the preliminary phase, its potential is readily apparent. Hence, it is the recommendation for the next study to improve upon the method and, if possible, to run a comparative study with already-known methods to determine the relative improvement introduced by this method.

## ACKNOWLEDGEMENTS

The authors would like to thank PetroChina Company Indonesia, especially the J.O.B. PPS (Joint Operating Body PERTAMINA-PetroChina

Salawati) for providing the opportunity to work together with the exploration team, and for providing the raw data needed to complete this study. All raw data, shown or not, are the properties of J.O.B. PPS and used with permissions after necessary removal of sensitive and identifying information. All results are properties of the authors and may be used for reference on any further studies as long as citing this paper correctly.

## REFERENCES

- Bredesen, K., 2012. *Use of inverse rock physics modeling in reservoir characterization. Thesis of Master Science*, Department of Earth Science, University of Bergen, 78pp.
- Candikia, Y.N., Rosid, M.S., and Haidar, M.W., 2017. Comparative Studies between Kuster-Toksoz and Differential Effective Medium (DEM) Method for Determining Pore Types in Carbonate Reservoir, *AIP Conference Proceedings*, 1862, 030185. DOI: 10.1063/1.4991289.
- Cheng, C.H. and Toksöz, M.N., 1979. Inversion of seismic velocities for the pore aspect ratio spectrum of a rock. *Journal of Geophysical Research: Solid Earth*, 84 (B13), p.7533-7543. DOI: 10.1029/JB084iB13p07533
- Choquette, P.W. and Pray, L.C., 1970. Geologic Nomenclature and Classification of Porosity in Sedimentary Carbonates. *AAPG Bulletin*, 54 (2), p.207-250. DOI: 10.1306/5d25c98b-16c1-11d7-8645000102c1865d
- Haidar, M.W., Wardhana, R., Iksan, M., and Rosid, M.S., 2018. Optimization of Rock Physics Models by Combining the Differential Effective Medium (DEM) and Adaptive Batzle-Wang Methods in "R" Field, East Java, *Scientia Bruneiana*, 17 (2), p.23-33. DOI: 10.46537/scibru.v17i2.78
- Kuster, G.T. and Toksöz, M.H., 1974. Velocity and Attenuation of Seismic Waves in Two-Phase Media: Part I. Theoretical Formulations.
- Lubis, L.A. and Harith, Z.Z.T., 2014. Pore Type Classification on Carbonate Reservoir in Off-shore Sarawak using Rock Physics Model and Rock Digital Images. *IOP Conference Series: Earth and Environmental Science*, 19 012003. DOI:10.1088/1755-1315/19/1/012003.
- Mavko, G., Mukerji, T., and Dvorkin, J., 2009. *The Rock Physics Handbook*. 2<sup>nd</sup> edition. New York: Cambridge University Press, pp.
- Nurhandoko, B.E.B., Djumhana, N., Iqbal, K., Rahman, I., Susilowati, and Hariman, Y., 2012. Fracture Characterization of Carbonate Reservoir Using Integrated Sequential Prediction of Artificial Neural Network: Case Study of Salawati Basin Field. *Proceedings of 36<sup>th</sup> Annual Convention and Exhibition, Indonesian Petroleum Association*.
- Osok, L.J.M.W., 2019. *Karakteristik Mikrofasies Batuan Karbonat Sebagai Reservoir Hidrokarbon Berdasarkan Data Outcrop Formasi Kais Cekungan Salawati Distrik Klayili, Kabupaten Sorong Propinsi Papua Barat. Master thesis*, Universitas Pembangunan Nasional Veteran Yogyakarta.
- Pamurty, P.G., Rochmad, Wibisono, A., Husein, S., Iqbal, K., Wasugi, M.D., and Al Hafeez, 2016. Identification of Fractured Basement Reservoir in SWO Field, Salawati Basin, West Papua, Based on Seismic Data: a New Challenge and Opportunity for Hydrocarbon Exploration in Pre-Tertiary Basement. *Proceedings of 40<sup>th</sup> Annual Convention & Exhibition, Indonesian Petroleum Association*. DOI: 10.1051/e3sconf/201912515002
- Prananda, A., Rosid, M.S., and Widodo, R.W., 2019. Pore Type and Porosity Distribution of Carbonate Reservoir Based on 3D Seismic Inversion in "P" Field Salawati Basin. *E3S Web of Conferences*, 125. DOI: 10.1051/e3sconf/201912515002
- Rosid, M.S., Wahyuni, S.D., and Haidar, M.W., 2017. Carbonate Reservoir Characterization with Pore Type Inversion using Differential Effective Medium (DEM) Model at X Field in East Java. *AIP Conference Proceedings*, 1862, 030179. DOI: 10.1063/1.4991283
- Rosid, M.S., Augusta, F.F., and Haidar, M.W., 2018. Integrated Analysis Seismic Inversion

- and Rockphysics for Determining Secondary Porosity Distribution of Carbonate Reservoir at "FR" Field. *IOP Journal of Physics: Conference Series*, 1013 (2018) 012175; DOI:10.1088/1742-6596/1013/1/012175
- Rosid, M.S., Kurnia, R.A., and Haidar, M.W., 2020. Estimation of 3D Carbonate Reservoir Permeability and Interparticle Porosity Based on Rock Types Distribution Model. *International Journal of GEOMATE*, 19 (74), p.59-65. DOI: 0.21660/2020.74.10910
- Satyana, A.H., Salim, Y., and Demarest, J.M., 1999. Significance of Focused Hydrocarbon Migration in the Salawati Basin: Controls of Faults and Structural Noses. *Proceedings of 27<sup>th</sup> Annual Convention and Exhibition, Indonesian Petroleum Association*. DOI: 10.29118/ipa.346.g.107
- Satyana, A.H., Purwaningsih, M.E.M., and Ngantung, E.C.P., 2002. *Evolution of the Salawati Structures, Eastern Indonesia: A Frontal Sorong Fault Deformation*. Surabaya, Indonesian Association of Geologists.
- Verwer, K., Eberli, G., Baechle, G., and Weger, R., 2010. Effect of carbonate pore structure on dynamic shear moduli. *Geophysics*, 75 (1), E1-E8. DOI: 10.1190/1.3280225
- Wang, Z., 2001. Fundamentals of Seismic Rock Physics. *Geophysics*, 66 (2), p.398-412. DOI: 10.1190/1.1444931
- Xu, S. and Payne, M.A., 2009. Modeling Elastic Properties in Carbonate Rocks. *The Leading Edge*, 28 (1), p.66-74. DOI: 10.1190/1.3064148
- Xu, S. and White, R. E., 1995. A new velocity model for clay-sand mixtures. *Geophysical Prospecting*, 43, p.91-118. DOI: 10.1111/j.1365-2478.1995.tb00126.x
- Ye, L.J. and Hong, C.X., 2013. A rock-physical modeling method for carbonate reservoirs at seismic scale. *Applied Geophysics*, 10 (1), p.1-13; DOI:10.1007/s11770-013-0364-6.
- Zhao, L., Nasser, M., and Han, D.H., 2013. Quantitative Geophysical Pore-Type Characterization and its Geological Implication in Carbonate Reservoirs. *Geophysical Prospecting*, 24 61 (4), p.827-841. DOI: 10.1111/1365-2478.12043